CALIBRATION OF ACOUSTIC EMISSION SENSORS

P. Kolář [1], M. Petružálek [2]

[1] Institute of Geophysics CAS, [2] Institute of Geology CAS

Abstract

Measurement of acoustic emission (AE) during laboratory experiments – rock sample loading - is an important tool for study of material mechanical properties as well as understanding of modes of its failure. For correct data processing it is necessary to calibrate used AE sensors; the calibration constants can depend on property of individual sensors, on their contact conditions, etc. As there can be a deformation induced charge in sensor contact condition, the calibration constants may vary with time.

AE sources can be modeled (in the same way as natural earthquakes) as double couple sources with use of moment tensor (MT) formalism (3x3 symmetric tensor, i.e. 6 independent values, the problem is linear). We adopted method, which enable calibration of an individual station of a seismic network. The method is based on simultaneous determination of MTs and calibration constant(s). During the experiment there were repeatedly measured velocities of elastic waves by ultrasonic sounding, when AE sensors cyclically acted as sources. We processed this data and for each cycle determined calibration constant for all the sensors but one, which is supposed to be 1. The source is supposed to be of single force type, which further reduces number of determined parameters. The evaluation was performed cyclically for all the sensors, the final calibration constants are then the mean values.

1 Introduction

Laboratory loading experiments are an effective way to study material properties. Important information is recorded by acoustic emission (AE) sensors, which are distributed on sample surface. At the certain level of stress, the microcracking in material begins. The microcraking is accompanied by emission of seismic waves, which are called acoustic emission (AE). The AE wave carries the information about its source as well as about the material through which it is going. Using the AE sensors, this information may be recorded as an AE waveform, which can be analyzed further. Such experiments can be also used to model destructive processes in rock which are in nature manifested as earthquakes. During such experiments we have to suppose scaling law validity over many orders, but in laboratory experiments many of material and process characteristics can be measured, controlled or directly evaluated to the contrary to the natural processes. In present, the loading laboratory experiments play an important role in understanding of earthquakes.

Obviously laboratory experiments differ from natural observations in many details and the methodology of earthquakes data processing cannot be applied directly. One of the partial tasks which must be solved to process successful laboratory experiments is AE sensors calibration. The calibration constants (CC) can depend on property of individual sensors, on their contact conditions, etc.; constants may vary when the condition change. To calibrate AE sensors we modified method originally designated to recalibrate a station of a seismic network proposed by (Davi and Vavryčuk 2012).

2 Basic ideas

A seismic source can be effectively described by moment tensor (MT) formalism, such approach is widely and routinely used for events from micro- to macro-scales (Dziewonski et al. 1981; Julian et al. 1998). MT is of 3x3 size, is symmetric, i.e. it has only 6 independent component. It can be determined from equation

$$\mathbf{G}\,\mathbf{m} = \mathbf{u}\,, \tag{1}$$

where $\boldsymbol{G}$ are Green's function amplitudes of Nx6 size, N is number of stations or number of observations respectively, $\boldsymbol{m}$ are components of MT, here transformed into 6x1 size vector and $\boldsymbol{u}$ are

observed data (Nx1 size vector). Under such configuration, the problem is linear and there are many tools for its effective solution.
Formally two different MT can be evaluated simultaneously for two events from equation

$$\begin{bmatrix} \boldsymbol{G}^1 & \mathbf{0} \\ \mathbf{0} & \boldsymbol{G}^2 \end{bmatrix} \begin{bmatrix} \boldsymbol{m}^1 \\ \boldsymbol{m}^2 \end{bmatrix} = \begin{bmatrix} \boldsymbol{u}^1 \\ \boldsymbol{u}^2 \end{bmatrix} \quad , \tag{2}$$

where $\boldsymbol{G}^i$ is $\boldsymbol{G}$ for ith event, i = 1, 2 and analogously for $\boldsymbol{m}^i$ and $\boldsymbol{u}^i$. Let suppose now, that k^{th} station of the network is wrongly calibrated. It can happened e.g. if a logger amplification was switched but not documented (e.g. during unplanned exchange of broken device etc.). In such a case each u^i_k component must be multiplied by C_k constant, which is unknown. It can be determined in a following way: we can put k = 1 without losing generality, as the station numbering can be shifted cyclically. Unknown C_1 can be evaluated by solving

$$\begin{bmatrix} \boldsymbol{G}^{1*} & \mathbf{0} & 0 \\ \mathbf{0} & \boldsymbol{G}^{2*} & 0 \\ \boldsymbol{G}^1_1 & \mathbf{0} & -u^1_1 \\ \mathbf{0} & \boldsymbol{G}^2_1 & -u^2_1 \end{bmatrix} \begin{bmatrix} \boldsymbol{m}^1 \\ \boldsymbol{m}^2 \\ C_1 \end{bmatrix} = \begin{bmatrix} \boldsymbol{u}^{1*} \\ \boldsymbol{u}^{2*} \\ 0 \\ 0 \end{bmatrix}, \tag{3}$$

where $\boldsymbol{G}^{i*} = \boldsymbol{G}^{i}_{(2:N,\ 1:6)}$, i.e. Green's function coefficients for all but the first station; and analogously $\boldsymbol{u}^{i*}$; the first station data are considered by lower matrix part by $\boldsymbol{G}^{i}_{1} = \boldsymbol{G}^{i}_{(1,\ 1:6)}$ and analogously for u^i_1. The method can be extended for more events and up to L uncalibrated stations (L <= N-1), but the problem must remain over-determinate. The general version of the equation system is given in (Davi and Vavryčuk 2012).

3 Rock material and experimental setup

As a "model rock" the Westerly granite was used in our study. Westerly granite, probably the most tested granitic rock, was used as an experimental rock material due to its homogeneity and a small grain size (<0.2mm); mechanical and descriptive properties of the material are given in (Petružálek et al. 2017).

The specimen in the shape of octagonal prism was grinded from the original cylindrical one. The specimen has 52 mm in diameter and height of 104 mm. Usage of the prismatic shape of specimen, compare to the cylindrical one, improves the sensitivity of ultrasonic methods due to the flat contact between surface of the specimen and AE sensor.

The specimen was uniaxially loaded in servo-hydraulic loading frame MTS 815. The loading was controlled by the linear combination of axial stress and axial strain (Okubo and Nishimatsu 1985). Two axial MTS extensometers measured the axial strain. The lateral strain was measured by the tensometric cantilever (Ergotech). Both strain gauges were attached directly to the specimen. 14 broadband acoustic emission sensors (Fuji) with 8 mm in diameter were attached to the surface of the specimen. All the sensors were used for acoustic emission (AE) monitoring as well as for ultrasonic sounding (US); Fig. 1 shows an experimental setup with all the attached sensors.

A high-voltage sine pulse (200 V) with a frequency of 200 kHz was used as a source of US. This corresponds to wavelengths of 2 - 3 centimeters for velocities from 4 to 6 km/s. The AE and US waveforms were recorded by a multi-channel transient recorder (Vallen System AMSY - 5, Germany). This apparatus was set up in triggered regime, the sampling rate was 10 MHz and the length of recorded waveforms was 1024 points, each point with 16 bit resolution of the A/D converter.

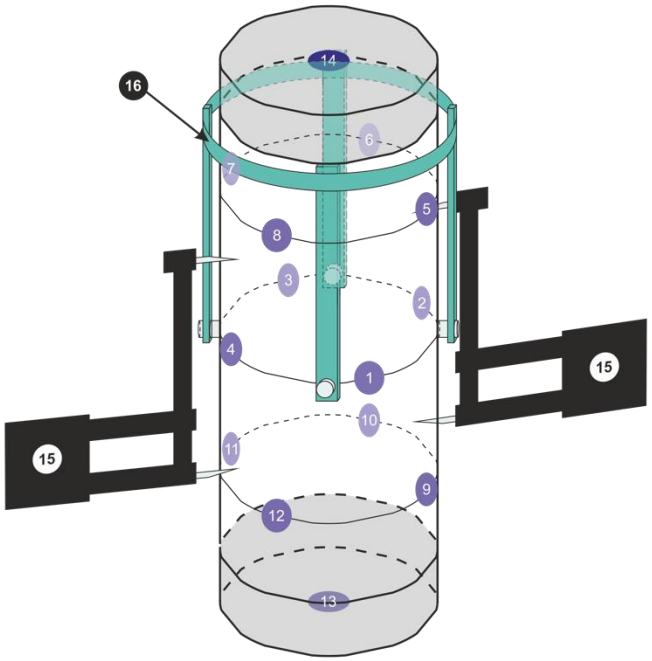

Figure 1. Experimental setup: 1-14 - AE/US sensors Fuji AE204; 15-extensometer MTS 632.11D-90; 16-cantilever Ergotech

4 Data

During the experiment there were continuously recorded signals from 14 AE/US sensors. These signals were lately processed: there were found about 21000 AE events of which more than 6000 stronger were localized using grid search method with anisotropic velocity model (Petružálek et al. 2013), the localization error should not exceed 3mm.

The piezocermic AE sensors were used for periodical ultrasonic sounding during the loading experiment as well. It was realized in a cycle(s), where step by step each sensor acted as a transmitter while the rest of them were receiving the transmitted ultrasonic waves. The prime purpose of this measurement was to determine stress dependency of anisotropic velocity and attenuation. The evolution of P wave velocity anisotropy, during the uniaxial loading experiment, is depicted in Fig. 2. The vertical and horizontal velocity were almost the same before the loading. Above 90 % of failure strength, there is a velocity difference of 1.3 km/s, which means about 26% anisotropy.

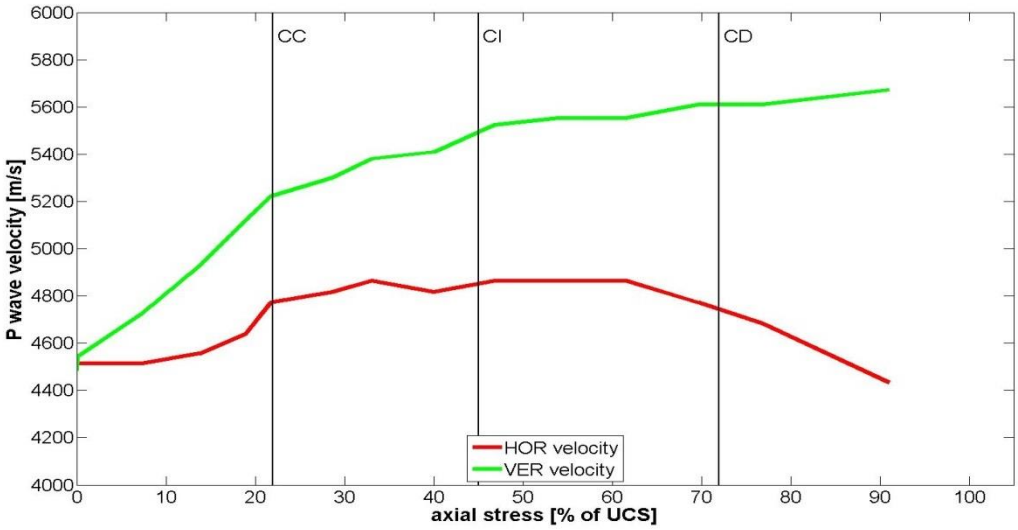

Figure 2. P wave velocity anisotropy, green color – vertical direction, red color – horizontal direction, CC - crack closure, CI – crack initiation, CD – crack damage.

5 Sensors calibration

An attempt of sensors calibration with use of AE events, based on approach by (Davi and Vavryčuk 2012) was unsuccessful – the calibration was unstable. Therefore we decided to use data from US measurement. For the purpose of sensors calibration, we consider one set of calibrating measurement as a set of 14 events recorded by 13 stations (14 - 1). The location of US events are and are identical with the sensor positions. For each set of US measurement the sub-calculations are performed in a loop: for each US source one of the AE sensors is cyclically supposed to have calibration constant equal 1, while the others are calibrated; the final calibration value is then evaluated as a mean of this sub-calibrations. Calibrations are evaluated with use of generalized form of eq. [3], each time for 13 events and 12 (14 - 1 - 1) calibrated sensors.

6 Amplitude correction for medium influence

The influence of medium on the raw data has to be corrected before evaluation of CC is performed. We consider two medium models: (i) semi-homogeneous: homogeneous model but with anisotropic wave velocity variation and (ii) anisotropic medium model.

Wave velocities periodically measured during the experiment exhibit relatively strong anisotropy, namely in the latest experiment phase; we suppose homogeneous elliptic distribution of velocities with principal axe oriented in vertical direction and equal horizontal axes.

Semi-homogeneous model

The semi-homogeneous model is defined by equation 4.92 (Aki and Richards 2009)

$$\mathbf{u_P}(R) = \frac{F^P \mu A}{4 \pi \rho v_P^3 R} \dot{\mathbf{u}} \ , \tag{4}$$

where displacement $\boldsymbol{u_P(R)}$ of P wave in distance R from the source depends on F^P P wave radiation pattern, density ρ, P wave velocity v_P, rigidity μ, fault area A and average source displacement $\dot{\bar{\boldsymbol{u}}}$; as the constants are not important in our case, only distance R and velocity v_P play the role. The v_P velocity is taken from the elliptic velocity model different for each source – sensors pair, but then the homogeneous model is applied. The correction is extended for attenuation correction: we suppose acausal model described as

$$A_1 = A_0 \ \ exp\left(\frac{-2 \pi f t_P}{2 Q_P}\right) \ , \tag{5}$$

where A_1 is attenuated amplitude A_0, f is frequency (f = 0.5 MHz in our case), t_P is P wave travel time and Q_P is attenuation coefficient (we put Q_P = 80) (Aki and Richards 2009).

Anisotropic model

The anisotropic model is described by the equations given in (Stierle et al. 2016). Used formulas in form of MATLAB code are given in App. 1.

For both models we suppose only isotropic type of source (transformation from single force type source through angle of incident). This enable reduce number of determined MT components (from 6 to only 3 isotropic), which is additional simplification of the system of equation to be solved. In addition free surface coefficients given in (Červený et al. 1977) are applied. These coefficients are applied two times: on the source side and on the receiver side.

7 Results

Results of calibration are given in graphical form in Fig. 3. For both models it is problematic sensor 11, probably due to wrong fixation[1]. Sensors 13 and 14 are placed in the press bits and their contact condition can improve with increasing load at the beginning of the experiment. The coefficients for anisotropic model are practically constant for principal part of the experiment – therefore we conclude that this model is more adequate.

Optionally, the method can be extended and in addition to the CC can be simultaneously determined also absorption quality factors – details are given in App. 2.

[1] The problem with sensor No. 11 fixation was noticed already during the experiment, but for technical reason the sensor couldn't be re-fixed.

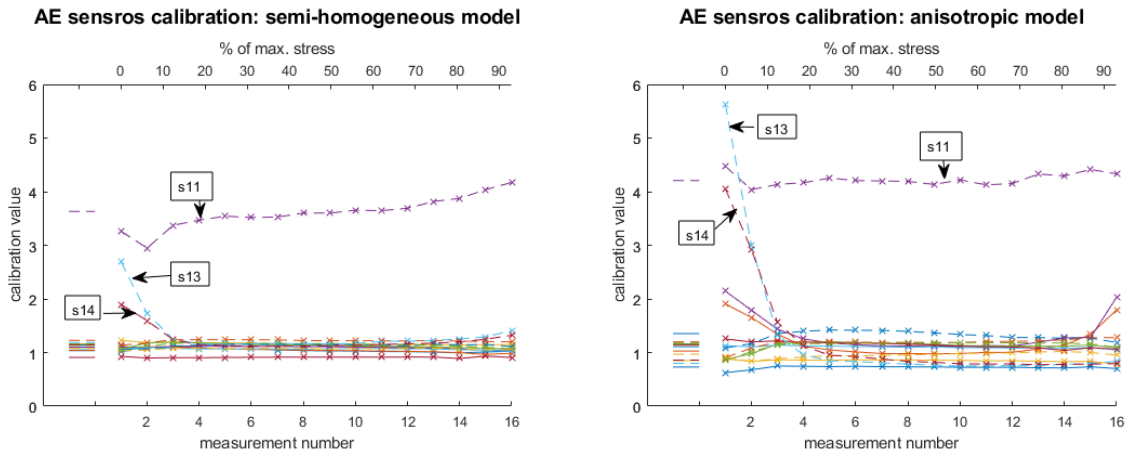

Figure 3. Calibration constants for 14 sensors in 16 measurements (times) for two considered medium models. Short lines on the left indicate average values from measurements 4-15 used in further AE processing. Sensor s11 exhibits significantly higher calibration value, probably due to poor contact condition. Contact condition of sensors s13 and s14 improve at the beginning of the experiment as they are located in the steal bits of the press.

8 Conclusion

We propose a new method for AE sensors calibration which exploits data from active ultrasonic sounding primary performed to determine wave velocities in the sample. The method is based on simultaneous evaluation of the source mechanism and calibration constants. The method yields stable and reasonable results even in the cases when calibration based on AE data were unsuccessful; the obtained calibration constants can be used for further processing of acoustic emission events.

Acknowledgement

We are thankful to V. Vavryčuk for kind consultation of anisotropic model usage.

The work was supported by grant GAČR 16-03950S P108 and Scientific Programme RVO67985831 of the Institute of Geology.

References

Aki K, Richards PG (2009) Quantitative seismology 2nd. University Science Book, Sausalito

Červený V, Molotkov IA, Pšenčík I (1977) Ray Method in Seismology. Charles Univesity press, Prague

Davi R, Vavryčuk V (2012) Seismic Network Calibration for Retrieving Accurate Moment Tensors. Bull Seismol Soc Am 102:2491–2506. doi: 10.1785/0120110344

Dziewonski AM, Chou T-A, Woodhouse JH (1981) Determination of earthquake source parameters from waveform data for studies of global and regional seismicity. J Geophys Res Solid Earth 86:2825–2852. doi: 10.1029/JB086iB04p02825

Julian BR, Miller AD, Foulger GR (1998) NON-DOUBLE-COUPLE EARTHQUAKES 1. THEORY. Rev Geophys 36:525–549.

Okubo S, Nishimatsu Y (1985) Uniaxial compression testing using a linear combination of stress and strain as the control variable. Int J Rock Mech Min Sci Geomech Abstr 22:323–330. doi: 10.1016/0148-9062(85)92064-9

Petružálek M, Lokajíček T, Svitek T (2017) Ultrasonic method for estimation of crack initiation stress.

51st US Rock Mech. / Geomech. Symp.

Petružálek M, Vilhelm J, Rudajev V, et al. (2013) Determination of the anisotropy of elastic waves monitored by a sparse sensor network. Int J Rock Mech Min Sci 60:208–216. doi: 10.1016/j.ijrmms.2012.12.020

Stierle E, Vavryčuk V, Kwiatek G, et al. (2016) Seismic moment tensors of acoustic emissions recorded during laboratory rock deformation experiments: sensitivity to attenuation and anisotropy. Geophys J Int 205:38–50. doi: 10.1093/gji/ggw009

P. Kolář
Contact information: Institute of Geophysics, CAS, Boční II / 1401, Prague 4, kolar@ig.cas.cz

M. Petružálek
Contact information: Institute of Geology, CAS, Puškinovo náměstí 447, Prague 6, petruzalek@gli.cas.cz

Appendix 1

General anisotropic model is described by the equations given in (Stierle et al. 2016). As for our task only signal amplitudes are relevant and signal phases can be omitted, the formulas can be rewritten into following form of MATLAB code:

```
%
% amplitude correction coefficients (ACCa)
% for Anisotropic model
%
  for i=1:nJevu
     a11=vh(i).^2 .*(1-1i./Qh1);              % [E13]
     a33=vv(i).^2 .*(1-1i./Qv1);              % [E13]

     X1=X(i,:);
     Y1=Y(i,:);
     Z1=Z(i,:);

     Nxyz=sqrt(X1.*X1 + Y1.*Y1 + Z1.*Z1);
     X1=X1./Nxyz;
     Y1=Y1./Nxyz;
     Z1=Z1./Nxyz;

     Nrm1 = sqrt(a33*X1.*X1 + a33*Y1.*Y1 + a11*Z1.*Z1);
     Nrm  = repmat(Nrm1',1,3);
     P0= ([X1'*a33/a11 Y1'*a33/a11' Z1'*a11/a33])./Nrm;  % [E9]
     Ann1 = [a11 a11 a33];
     Ann = repmat(Ann1,nSnimacu,1);
     V = Ann .* P0;                           % [E10]
     Vvel = sqrt(sum(V.*V,2));                % [E12]
     Kaz =  a11*a11*a33 ./ (Vvel.^4);         % [E11]
     vAnz(i,:) = abs(dot(P0,[X1' Y1' Z1'],2) ./ (Vvel.*sqrt(abs(Kaz))));
  end

  ACCa = 1/(4*pi*ro) ./ Xd  .* vAnz;          % [E11]
```

where nJevu is number of events, nSnimacu is number of sensors, vh and vv is actual horizontal and vertical waves velocity, X, Y and Z are ray vectors, dimension of X(nJevu, nSnimacu) and analogously for Y and Z; Qh1 and Qv1 are horizontal and vertical Q-factors, Xd are source-receiver distances (the same dimension as X), ro is density; notification [Enn] refers to formula numbers used in (Stierle et al. 2016).

Appendix 2

In addition to the determination of CC we extended the method and simultaneously determined also attenuation $A_{H/V}$. We repeatedly evaluated CC for all possible combination of A_H and A_V (i.e. grid search was performed) and as their most probable values we chosen the combination with lowest RMS of the problem.

The Q-factor $Q_{H/V}$ and absorption $A_{H/V}$ are bounded by relations

$$Q_H = \frac{1}{2\,A_H\,V_H} \quad and \quad Q_V = \frac{1}{2\,A_V\,V_V} \quad , \tag{A1}$$

where $V_{H/V}$ are horizontal/vertical wave velocities (Stierle et al. 2016). An example of RMS distribution for one measurement is given in Fig. 3, determined absorption for the experiment is then in Fig. 4. The obtained results are preliminary and have to be verified.

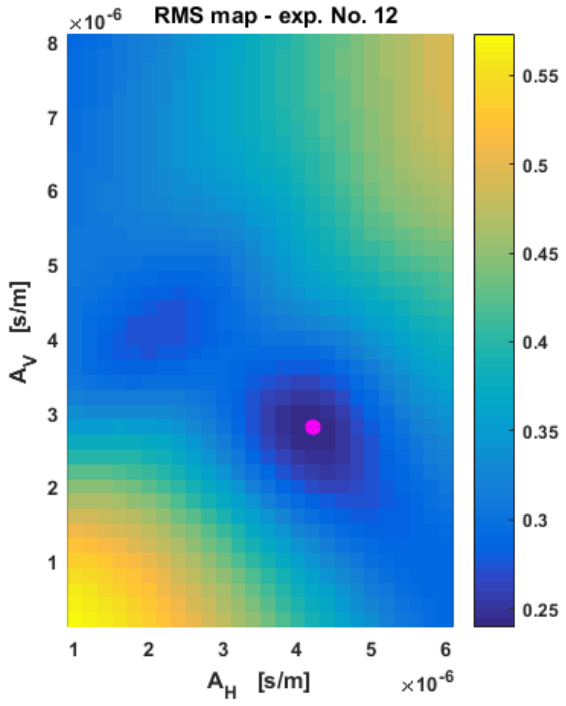

Figure 3: An example of RMS map for measurement No. 12, the minimum RMS position is marked by pink dot. All 16 measurements were processed in the same way.

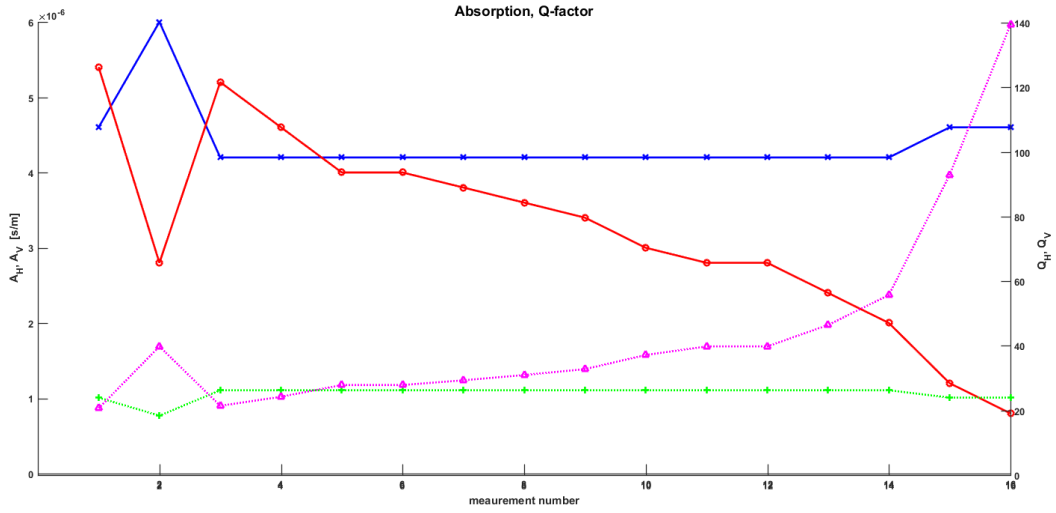

Figure 4. Determined values of absorption $A_{H/V}$ and Q-factor $Q_{H/V}$. A_H is marked by green color A_V by pink; Q_H by blue, Q_V by red. Again measurement No. 2 exhibits abnormality which we interpret as an error.